Primljen / Received: 26.7.2022.
Ispravljen / Corrected: 27.4.2023.
Prihvaćen / Accepted: 30.4.2023.
Dostupno online / Available online: 10.8.2023.

Influence of clay mineralogy on undrained shear strength using Fall cone test

Author:

Assoc.Prof. Eyyüb Karakan, PhD. CE
Kilis 7 Aralik University, Kilis, Turkey
Department of Civil Engineering
eyyubkarakan@kilis.edu.tr
Corresponding author

Original research paper

Eyyüb Karakan

Influence of clay mineralogy on undrained shear strength using Fall cone test

Consistency limits are the basic parameters used as standard inputs for any soil investigation program to evaluate the geotechnical properties of fine-grained soils. The primary objective of this study is to investigate the variations in the undrained shear strength of clays with different plasticity properties based on the fine content, clay mineralogy, and water absorption capacity. To achieve this objective, 33 Fall cone tests were conducted on low-, high-, and very high-plastic clay mixtures. Various blends of different plasticity were ensured by preparing mixtures of Na-montmorillonite (NaM)/Ca-montmorillonite (CaM), Na-montmorillonite (NaM)/Kaolinite (K), and Na-montmorillonite (NaM)/Sepiolite (S). According to the experimental results, the highest liquid limit (LL) was obtained in 100 % NaM clay at 255.07 %, whereas the lowest LL was obtained in 100 % S clay at 33.55 %. Similarly, the highest undrained shear strength was obtained at 160 kPa at 30 % water content in the 100 % NaM clay, whereas the lowest undrained shear strength was obtained at 10 kPa in the 100 % S clay at the same water content. Consequently, based on an experimental framework, empirical equations were obtained which could be used to establish the relationships among cone penetration-water content, liquid limit-clay content, and undrained shear strength-cone penetration.

Key words:
Atterberg limits, undrained shear strength, clay mineralogy, fall cone test

Izvorni znanstveni rad

Eyyüb Karakan

Utjecaj mineralogije gline na nedreniranu posmičnu čvrstoću pomoću pokusa s padajućim šiljkom

Granice konzistencije su osnovni parametri koji se primjenjuju kao standardni ulazni podaci za bilo koji program istraživanja tla za procjenu geotehničkih svojstava sitnozrnatog tla. Primarni je cilj ovog rada istražiti varijabilnost u nedreniranoj posmičnoj čvrstoći glina s različitim svojstvima plastičnosti na temelju udjela finih čestica, mineralogije gline i sposobnosti apsorpcije vode. Kako bi se postigao taj cilj, provedena su 33 pokusa s padajućim šiljkom na mješavinama gline niske, visoke i vrlo visoke plastičnosti. Različite mješavine različite plastičnosti osigurane su pripremom smjesa Na-montmorilonita (NaM)/Ca-montmorilonita (CaM), Na-montmorilonita (NaM)/kaolinita (K), i Na-montmorilonita (NaM)/sepiolita (S). Prema eksperimentalnim rezultatima, najviša granica tečenja (LL) dobivena je u 100 % NaM gline pri 255,07 %, dok je najniža LL dobivena u 100 % S gline pri 33,55 %. Najveća nedrenirana posmična čvrstoća dobivena je na 160 kPa pri 30 % vlažnosti u 100 % NaM gline, a najmanja nedrenirana posmična čvrstoća dobivena je na 10 kPa pri 100 % S gline pri istoj vlažnosti. Stoga, na temelju eksperimentalnog okvira, dobivene su empirijske jednadžbe koje se mogu primijeniti za utvrđivanje odnosa između prodiranja šiljka i vlažnosti, granice tečenja i udjela gline te nedrenirane posmične čvrstoće i prodiranja šiljka.

Ključne riječi:
Atterbergove granice, nedrenirana posmična čvrstoća, mineralogija gline, pokus s padajućim šiljkom

1. Introduction

Generally, clay minerals have an extremely small size and a crystalline structure that is electrochemically very active. Therefore, the same amount of clay can cause significant changes in the engineering properties of soils owing to their different mineralogical properties. If the clay percentage ranges between 25–35 %, most of the coarse-grained particles (sand or gravel) in the soil will float in the matrix formed by the clay, and such coarse-grained particles slightly influence the overall engineering behaviour [1]. Another important feature of clay soils is that, while the presence of water significantly affects the overall behaviour of clays, its effect of the grain size distribution is less significant. Conversely, the grain shape and size significantly affect the behaviour of coarse-grained soils, whereas the effect of water on such soils is less important. As shown in Figures 1a. to 1.d (Ca-Montmorillonite/ Na- Montmorillonite (*CaM-NaM*), scanning electron microscopy (SEM) analysis), montmorillonite crystals can be extremely small but exert remarkably high attractive forces. With an increasing water content of clays with montmorillonite, the swelling potential between the layers increases considerably. Clays with different mineralogical properties, such as montmorillonite and bentonite, have different charge balances and thus have different tendencies to attract exchangeable cations [2]. This explains the substantially higher affinity of montmorillonite clay for exchangeable cations than kaolinite.

The structure of fine-grained soil significantly influences the engineering behaviour. The stress path influences the formation of combinations of natural clay blends. The relationship between the micro and macro behaviours of clays has been investigated by many researchers to date [2–6]. In soil, structure is defined to include the texture or geometrical arrangement of grains and/or mineral particles and the forces between the grains. In this case, the soil texture defines only the geometric arrangement of the grains. Because the surface activity of each grain is extremely low in coarse-grained soils, the intergranular forces are also extremely low. Therefore, the definitions of texture and structure are the same for coarse-grained soils. In contrast, the intergranular forces in clay soils are quite high; therefore, both intergranular forces and soil texture are complementary definitions.

The primary objective of this study is to examine how the undrained shear strengths of clays with different mineralogical properties are affected by the clay soil physical properties. These physical properties include water content, water content ratio, Atterberg limits, liquidity index, and log liquidity index. In this context, the Atterberg limits for different clay mixtures with three different plasticity levels and those reported in literature were evaluated. Subsequently, the data obtained in the experimental study and the results of previously published studies were compared to elucidate the behaviour of clays with different mineralogical properties. The relationships between the undrained shear strength, Atterberg limits, clay content, and type were evaluated in detail.

Abbreviation and notation list in this paper

β	- The slope of the fit straight line
A	- Activity
C_o	- The water content intercept at d=1 mm
CF	- Clay fraction
d	- Fall cone penetration [mm]
K	- Cone factor
I_L	- Liquidity index
I_{LN}	- Logarithmic liquidity index
LL	- Liquid limit [%]
m	- Mass (80 g)
PL	- Plastic limit [%]
PI	- Plasticity index [%]
R_p	- Plasticity ratio (PL/LL)
R^2	- Coefficient of determination
R_s	- Strength ratio
P_r	- Plastic ratio (PI/PL)
S_u	- Undrained shear strength[kPa]
S_{uLL}	- Undrained shear strength at the liquid limit [kPa]
S_{uPL}	- Undrained shear strength at the plastic limit [kPa]
S_t	- Sensitivity ratio
w	- Water content [%]
WCR	- Water content ratio

2. Literature review

According to British Standard BS1377-1990 [7], the 20 mm cone penetration depth in the Fall cone test is defined as the liquid limit (LL) of fine-grained soils. Many researchers [8–17] recommend universal adoption of Fall cone tests universally to define the LLs of clays. In this study, the water content required for 2-mm cone penetration in Fall cone tests, as suggested by Hansbo [18], was accepted as the plastic limit (PL). Wroth and Wood [19] showed that $(S_u)_{PL}/(S_u)_{LL}$ was 100. Nagaraj et al. [10] experimentally obtained the S_u values corresponding to the water content at the LL are not constant. Nagaraj et al. [10] observed that the calculated S_u values differed when different methods were used. The Fall cone test method can be used to obtain S_u values in many soils, such as CH, CL, ML, and MH soils. Equation (1) was proposed by Hansbo [18] to calculate the undrained shear strength, S_u [kPa] of fine-grained soils using the Fall cone test.

$$S_u = K \cdot \left(\frac{mg}{d^2} \right) \text{[kPa]} \tag{1}$$

where K is the cone factor (0.867), m is the mass (80 g), g is the gravitational acceleration (9.8 m/s^2), and d is the Fall cone penetration (mm). The relationship between the water content, liquidity index, and undrained shear strength of the soil has been studied by many researchers [11, 12, 20]. However, a log-log plot of liquidity index and undrained strength will inevitably achieve undefined values as the PL is approached, as log 0 → -∞.

Koumoto and Houlsby [21] explain that if a power model is used, then a 'logarithmic liquidity index' must be defined. The liquidity index (I_L) and logarithmic liquidity index (I_{LN}) are calculated using Equation (2) and Equation (3), respectively. The liquid and plastic limits of the soils were used to calculate the plasticity index, which can be empirically correlated with many soil properties. The plasticity index was used to predict the undrained shear strength of the soil. The undrained shear strength of clay is related to the liquidity index I_L, which is defined in Equation (2). The liquidity index is an identifier of the consistency of soils and can be empirically associated with the undrained shear strength, dynamic properties, and compression characteristics. Thus, consistency also plays a significant role in the selection of models used in modelling of stress-strain behaviour. Moreover, a semi-logarithmic model can be used to establish a generalised equation between the undrained shear strength and the liquidity index. An analysis of experimental results revealed that the data did not demonstrate a linear behaviour; therefore, a double logarithmic axis should be used for the linearisation of the data. However, a log-log plot of the liquidity index and undrained shear strength will inevitably be unidentified as the PL approaches zero. Therefore, if a power model is used, the 'logarithmic liquidity index' must be defined as in Equation (3).

$$I_L = \frac{w - PL}{LL - PL} \tag{2}$$

$$I_{LN} = \frac{\ln(w / PL)}{\ln(LL / PL)} \tag{3}$$

Table 1. Dependence of undrained shear strength on physical properties of clays

Equation No.	Author's	Equation
1	Whyte [21]	$S_u = 1.6e^{4.23(1-I_L)}$
2	Federico [23]	$S_u = e^{5.25\left(1.161\frac{w}{LL}\right)}$
3	Locat & Demers [26]	$S_u = \left(\frac{19.8}{I_L}\right)^{2.64}$
4	Terzaghi et al. [34]	$S_u = 2(I_L)^{-2.80}$
5	Koumoto & Houlsby [21]	$S_u = e^{\left(\frac{1.070-I_{LN}}{0.217}\right)}$
6	Lee [29]	$S_u = 182.93e^{-2.3714\left(\frac{w}{LL}\right)}$
7	Berilgen et al. [30]	$S_u = 145e^{-2.86\left(\frac{w}{LL}\right)}$
8	Berilgen et al. [30]	$S_u = 28e^{-1.33 I_L}$
9	Edil & Benson [31]	$S_u = 144.9e^{-1.72 I_L}$
10	Edil & Benson [31]	$S_u = 191{,}4e^{-(0{,}33LL)}$
11	Shimobe [35, 36]	$S_u = 98.S_t.exp.\left[\ln\left\{\frac{0.4755}{\left(I_L + 0.5012(1-I_L)\right)}\right\} / 0.19\right]$
12	O'Kelly [37]	$\log S_u = \log(S_{uLL}) + \left(\frac{\log R_s}{\log\left(\frac{LL}{PL}\right)}\right) \cdot \log\left(\frac{1}{WCR}\right)$
13	Vardanega & Haigh [11]	$\log_{10}(S_{u,C}) = 2.662 - 2.432\left[\frac{w}{LL}\right]$
14	Cangir & Dipova [38]	$S_u = -41\ln(I_L)+19{,}41$
15	Kang et al. [39]	$S_u = 1{,}71(WCR)-4{,}1$
16	Sharma & Sridharan [40]	$\log(S_{u,C} / 1.7) = \log(1.04) - 4.9\log(WCR)$
17	Karakan et al. [17]	$S_u = 210.51e^{-4.516 I_L}$
18	Karakan et al.[17]	$S_u = 119.62e^{-4.533 I_L}$

Many researchers have obtained various forms of relationships between the water content, water content ratio, liquid limit, liquidity index, and consistency index based on the undrained shear strength using empirical equations [21–33]. These relationships are summarised in Table 1.

3. Material and methods

All the soils used in this study were formed from binary mixtures of highly plastic Na-montmorillonite (*NaM*) clay with Ca-montmorillonite (*CaM*), kaolinite (*K*), and sepiolite (*S*) clays. *NaM* was selected as the primary material for this study because it exhibits the highest plasticity and activity. The microstructural properties of *NaM, CaM, K* and *S* clays were determined through scanning electron microscopy–energy dispersive X-ray analysis (SEM–EDX). Figure 1 shows the SEM photographs of the *NaM, CaM, K,* and *S* clays used in this study. The chemical properties of the clays used in this study are summarised in Table 2. The grain size distributions of all the clays are shown in Figure 2.

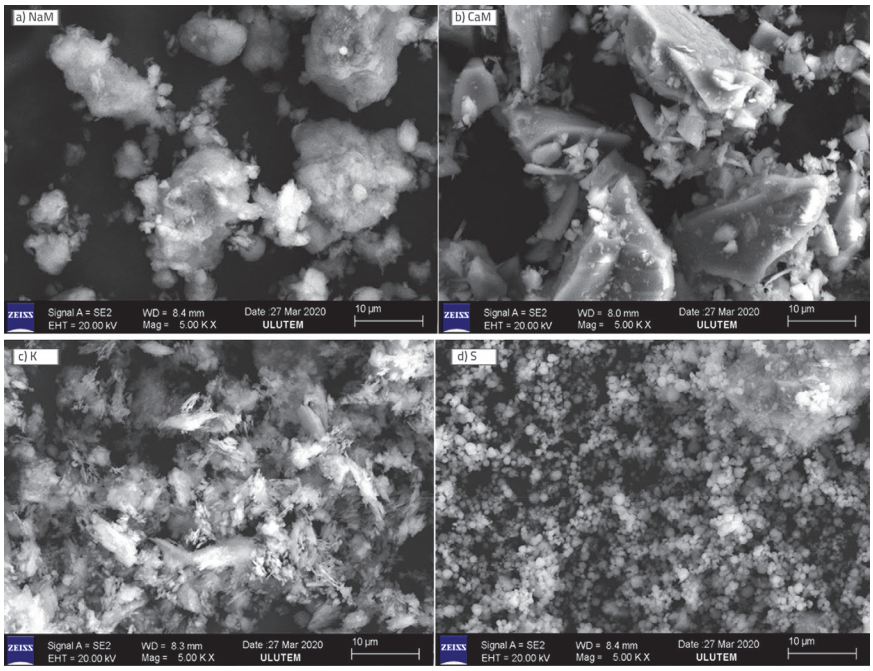

Figure 1. SEM photos of: a) Na-Montmorillonite (NaM); b) Ca-Montmorillonite (CaM); c) Kaolinite (K); d) Sepiolite (S)

Fall cone tests were conducted using equipment and procedures conforming to British standard BS 1377-1990 [7]. A standard specimen cup with a diameter of 55 mm and a depth of 40 mm was used. The water content was chosen such that penetrations were obtained between 5 and 30 mm for an 80-g cone with a 30° tip angle. According to BS 1377-1990 [7], the liquid limit of soil is defined as the water content corresponding to a cone penetration of 20 mm.

In this context, the Fall cone test was conducted to further evaluate the relationships between the physical properties (Atterberg limits, water content, water content ratio, liquidity index, and logarithmic liquidity index) and undrained shear strength of clay mixtures with different plasticity levels and mineralogical properties. All experiments were performed on binary mixtures, where the *NaM* content included in all the mixtures ranged from 0–100 % in 10 % increments. All the mixtures and the corresponding test results used in the experiments are listed in Table 3.

To demonstrate the reproducibility of the experimental results, significant efforts were made to prepare the test samples. A similar procedure was applied to the sample preparation method for all mixtures in the Fall cone tests. For the experiments, the clays were first dried in the oven for at least 24 h at 110 °C, then dry mixtures were prepared. Dry mixing was performed for at least 10 min until the mixture became completely homogeneous. Finally, water was added to the dry mixture and the mixture was maintained in a desiccator for 24 h.

Table 2. Chemical analysis of NaM, CaM, K, and S clays

Minerals	*NaM*	*CaM*	*K*	*S*
SiO_2	83	72.2	50.7	47
Al_2O_3	5.5	14	34	36
Fe_2O_3	0.2	0.7	0.6	0.6
TiO_2	0.05	0.05	0.8	0.8
CaO	0.4	1.1	0.6	0.6
MgO	2.10	3.2	0	1.4
Na_2O	0.15	0.25	0	0
K_2O	0.6	1	0	0
SO_3	0	0	0.3	0.6

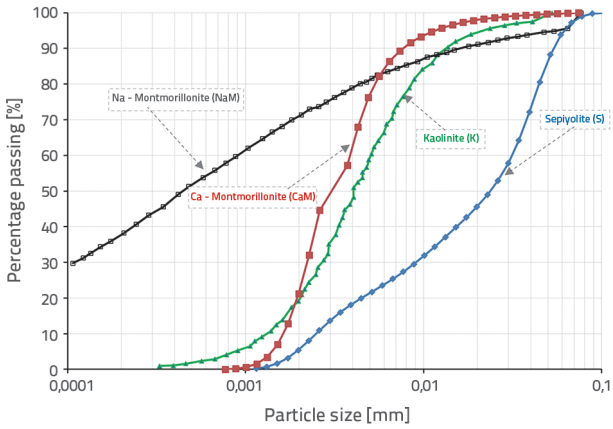

Figure 2. Grain size distribution of Na-Montmorillonite (NaM), Ca-Montmorillonite (CaM), Kaolinite (K), and Sepiolite (S)

4. Evaluation of experimental test results

4.1. Variation of cone penetration with water content

The cone penetration-water content relationship has been experimentally studied by several researchers to determine both the liquid and plastic limits of cohesive soils using Fall cone tests [17, 21, 41–44]. In such cases, a constant cone penetration value cannot be obtained for different types of soils (natural soils, sand-clay mixtures, sandy soils, and clay soils) with different water contents. Clays with different properties also exhibit different water absorption capacities in the liquid and plastic states. Therefore, clays with different mineralogical properties are not expected to have unique cone penetration values because of their different liquid and plastic limits [13–16, 21, 30, 45–47]. Figure 3 shows the cone penetration-

Table 3. Experimental test results

Mixture No.	NaM [%]	S [%]	K [%]	CaM [%]	LL_c [%] BS fall cone	PL_c [%] BS fall cone	$PI_c=LL_c-PL_c$	$R_{pc}=PL_c/LL_c$	$Pr_c=PI_c/PL_c$	$\tan\alpha_c=PI_c/(LL_c-20)$	Gs ρ_s [g/cm³]	Clay fraction,CF [%]	Activity (A)	C_0	β	R^2
1	100	0			255.07	68.99	186.08	0.270	0.371	0.792	2.350	71.35	2.61	15.304	0.900	0.994
2	90	10			204.49	62.94	141.55	0.308	0.445	0.767	2.355	64.75	2.19	12.264	0.938	0.991
3	80	20			183.80	58.39	125.41	0.318	0.466	0.766	2.360	58.15	2.16	10.608	0.949	0.990
4	70	30			174.05	52.60	121.45	0.302	0.433	0.788	2.365	51.55	2.36	8.922	0.983	0.973
5	60	40			162.41	49.32	113.10	0.304	0.436	0.794	2.370	44.95	2.52	7.434	1.028	0.997
6	50	50			142.50	47.27	95.23	0.332	0.496	0.777	2.375	38.35	2.48	7.652	0.970	0.976
7	40	60			103.89	39.33	64.57	0.379	0.609	0.770	2.380	31.76	2.03	15.935	0.635	0.974
8	30	70			82.42	38.36	44.07	0.465	0.870	0.706	2.385	25.16	1.75	16.407	0.554	0.967
9	20	80			62.82	37.65	25.17	0.599	1.496	0.588	2.390	18.56	1.36	21.847	0.369	0.979
10	10	90			54.48	34.66	19.83	0.636	1.748	0.575	2.395	11.96	1.66	25.138	0.271	0.949
11	0	100			33.55	30.51	3.04	0.909	10.023	0.225	2.400	5.36	0.57	25.719	0.095	0.969
12	100		0		255.86	67.42	188.44	0.264	0.358	0.799	2.350	71.35	2.64	27.519	0.759	0.990
13	90		10		252.38	64.50	187.88	0.256	0.343	0.809	2.360	66.31	2.83	25.742	0.768	0.986
14	80		20		239.56	65.26	174.30	0.272	0.374	0.794	2.370	61.27	2.84	26.286	0.749	0.973
15	70		30		239.56	65.85	173.71	0.275	0.379	0.791	2.380	56.22	3.09	20.934	0.793	0.987
16	60		40		193.40	60.58	132.81	0.313	0.456	0.766	2.390	51.18	2.59	22.236	0.734	0.991
17	50		50		180.89	51.47	129.42	0.285	0.398	0.804	2.400	46.14	2.80	21.011	0.727	0.991
18	40		60		154.47	49.84	104.63	0.323	0.476	0.778	2.410	41.10	2.55	16.522	0.755	0.991
19	30		70		121.08	48.69	72.39	0.402	0.673	0.716	2.420	36.06	2.01	18.224	0.646	0.974
20	20		80		99.18	41.03	58.15	0.414	0.706	0.734	2.430	31.02	1.87	18.461	0.573	0.980
21	10		90		70.30	39.17	31.13	0.557	1.258	0.619	2.440	25.97	1.20	22.638	0.392	0.967
22	0		100		58.20	38.36	19.84	0.659	1.934	0.519	2.450	20.93	0.95	23.057	0.322	0.969
23	100			0	255.57	68.00	187.57	0.266	0.363	0.796	2.350	71.35	2.63	31.213	0.693	0.955
24	90			10	239.71	66.35	173.36	0.277	0.383	0.789	2.350	66.34	2.61	31.405	0.688	0.941
25	80			20	224.65	65.96	158.69	0.294	0.416	0.775	2.350	61.32	2.59	19.373	0.823	0.969
26	70			30	217.91	55.57	162.35	0.255	0.342	0.820	2.350	56.31	2.88	20.992	0.792	0.969
27	60			40	207.24	53.32	153.92	0.257	0.346	0.822	2.350	51.30	3.00	20.859	0.772	0.907
28	50			50	196.56	52.27	144.29	0.266	0.362	0.817	2.350	46.29	3.12	16.442	0.834	0.926
29	40			60	184.84	51.96	132.88	0.281	0.391	0.806	2.350	41.27	3.22	20.396	0.748	0.964
30	30			70	176.27	50.98	125.30	0.289	0.407	0.802	2.350	36.26	3.46	20.110	0.606	0.905
31	20			80	166.02	49.74	116.28	0.300	0.428	0.796	2.350	31.25	3.72	21.554	0.688	0.918
32	10			90	150.79	47.04	103.74	0.312	0.453	0.793	2.350	26.24	3.95	20.317	0.680	0.891
33	0			100	148.28	47.97	100.31	0.324	0.478	0.782	2.350	21.22	4.73	21.698	0.648	0.877

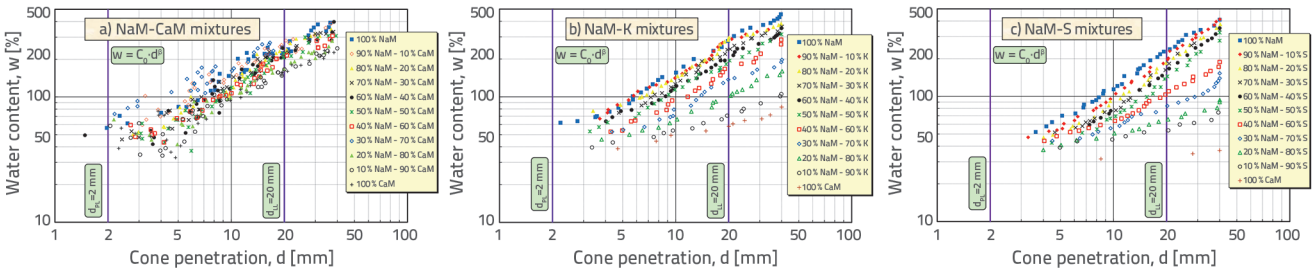

Figure 3. Cone penetration-water content relationship for a) NaM-CaM mixtures, b) NaM-K mixtures, c) NaM-S mixtures

water content relationships using Equations (4)–(6) based on the experimental results. The log-log relationship shown in Equation (5) and Equation (6), mixtures of *NaM-CAM, NaM-K,* and *NaM-S* for cone penetrations ranging from 1–40 mm, and the corresponding water contents ranging from 30–500 %, are shown in Figures 2.a to 2.c. Figures 3.a, 3.b and 3.c show that the coefficients of cone penetration seem to be dependent on the soil mineralogy, soil type, and soil plasticity.

The changes in cone penetration with water content for *NaM-CaM, NaM-K* and *NaM-S* mixtures on a bi-logarithmic scale are presented in Table 3 and Figures 3.a, 3.b, and 3.c. Because the *NaM-CaM* mixtures have an extremely high water content, they vary in a narrower band compared with the other two mixtures (Figure 3a). In the *NaM-CaM* mixtures shown in Figure 3a, the water content at 20 mm penetration varied between 180 % and 300 %. In contrast, in the *NaM-K* mixtures shown in Figure 3b, the change in water content with cone penetration was in a wider band range because of the lower water-holding capacity of kaolin clay.

When the water content is 300 % at 20-mm penetration for *NaM*, this value decreases considerably as the kaolinite content of the mixture increases; consequently, for 100 % *K* content, a value of 60 % is obtained. The same relationship for *NaM-S* mixtures is shown in Figure 3c; the decrease in water content is sharper compared to the other two mixtures. In this case, as the amount of sepiolite clay with the lowest water affinity increases by weight, water retention decreases considerably. Thus, the change in water content was within a wide range. Figure 3c shows that the water content corresponding to the same penetration for 100 % *S* decreases to approximately 35 %. This shows that the reduction in water retention capacity makes a significant difference for clay mixtures with different mineralogical properties.

LL tests of the clay mixtures used in this study were performed using a standard British cone [7]. The Fall cone test is preferred over the Casagrande method because both the liquid and plastic limit values can be determined together in Fall cone tests, and the results are more reproducible. The cone penetration (*d*) and water content (*w*) relationships were defined using Equation (4) as per Feng [42, 48]:

$$w = C_0 \cdot d^{\beta} \tag{4}$$

where C_0 is the water content intercept at d = 1 mm and β is the slope of the fitted straight line. The cone penetration corresponding to d_{LL} = 20 mm and d_{PL} = 2 mm show the liquid (LL_c) and plastic limit (PL_c) values of the BS cone [7], respectively. Therefore, the Fall cone liquid and plastic limit values are defined in Equations (5) and (6) as per [35]:

$$LL_c = C_0 \cdot (20)^{\beta} \tag{5}$$

$$PL_c = C_0 \cdot (2)^{\beta} \tag{6}$$

The coefficients C_0 and β for each mixture from Figures 3a, b, and c, which were obtained using Equations (5) and (6), and the corresponding R^2 values are presented in Table 3. For the *NaM-S* mixtures, the C_0 values vary between 7.434 and 25.719, and the β values vary between 0.095 and 1.028; the R^2 values obtained for *NaM-S* mixtures are minimum 0.949 and maximum 0.997. The C_0 values obtained of the *NaM-K* mixtures are at most 27.519, at least 16,522, while β values are at most 0.768 and at least 0.322. The R^2 values of the *NaM-K* mixtures are between 0.967 and 0.991. Finally, the C_0 values in the *NaM-CaM* mixtures were at least 16,442, with a maximum of 31,405, and the β values vary between 0.606 and 0.823. The R^2 values of the mixtures range from 0.877 to 0.969.

For the *NaM-S* mixtures, while the LL decreases continuously with increasing sepiolite content, the C_0 coefficient decreases from 15.304 to 7.434 and reaches its lowest value for the 60 %*NaM* and 40 %*S* mixture. The C_0 coefficient increases subsequently with increasing sepiolite content and reaches its highest value of 25.719 for 100 % sepiolite. Similar behaviour was observed in the *NaM-K* and *NaM-CaM* mixtures. The change in the β coefficient contradicted the change in the C_0 coefficient. For example, in *NaM-S* mixtures, the LL decreases continuously with increasing sepiolite content, whereas the β coefficient increases from 0.9 to 1.028 until the 60 %*NaM*-40 % *S* mixture is obtained. The β coefficient reaches its highest value in 60 %*NaM*-40 % *S* mixture, followed by a sharp decrease with increasing sepiolite content, and the lowest value of 0.095 was obtained for 100 % sepiolite.

Figure 4a shows that the LLs of *NaM-K* and *NaM-S* mixtures drastically increase and are parallel to each other as the *NaM* content increases. The LL values for pure sepiolite and kaolinite are 33.55 % and 58.2 %, respectively, and a value of 255.1 % is reached at 100 % *NaM* content. The increase in the LL value in the *NaM-S* mixtures was determined as (255.1 - 33.55 = 221.55 %), while the increase in the LL value in the *NaM-K* mixtures was calculated as (255.1 - 58.2 = 196.9 %). However, the rate of increase in the LL is lower in *NaM-CaM* mixtures than other mixtures because the mineralogical properties

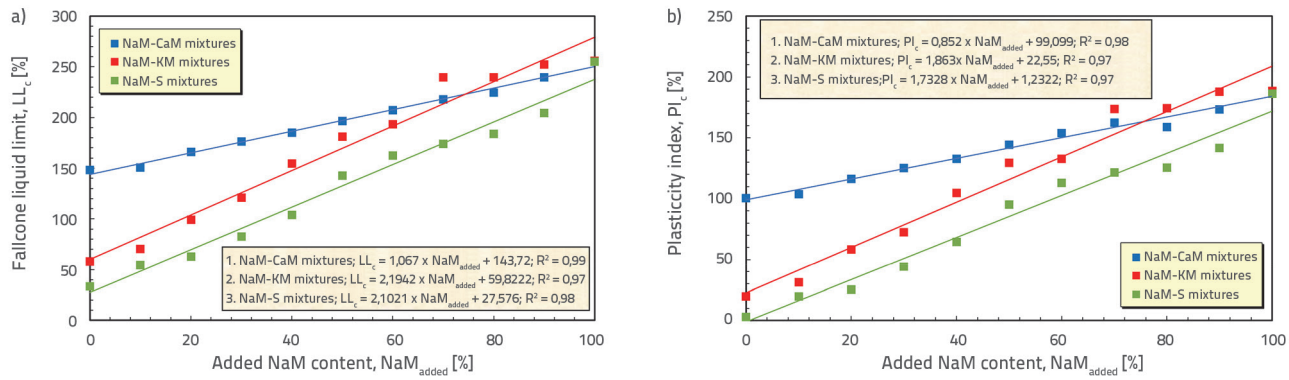

Figure 4. Effect of added NaM content with three different clay types (CaM, K and S) on a) the LL of mixture with clays and b) the plasticity index of mixture with clays

of *NaM* are considerably different from those of K and S, whereas its activity is higher than that of the other two clay minerals. The LLs of *CaM* and *NaM* are 148.3 % and 255.1 %, respectively. An increase in the LL from 148.3 % to 255.1 % caused an increase in the plasticity of the clay from high to very high. The plasticity index values are presented in Figure 4b. The effect of the increased *NaM* content on the plasticity index is evident. Adding 10 % *K* and *S* to *NaM* led to substantial increases in the plasticity index by approximately 25 % and 41 %, respectively. This was due to the high activity of the added *NaM* and its tendency to absorb water.

Because the activity of the soil varies according to the ratio between PI and CF, a PI value can be obtained as a function of CF [24]. The activity is influenced by many factors, such as the clay mineral type, absorbed cation type, pH, degree of crystallinity, and pure clay mineral content. The presence of kaolinite and montmorillonite in the soil provides a wider range of activity values when combined with these factors. The higher the activity of clay soils, the more important is the effect of the clay fraction on the intrinsic properties. Moreover, the activity is more sensitive to changes in the type of exchangeable cations and pore water composition. In this study, the activity values of *S, K, NaM,* and *CaM* can be arranged from high to low, respectively. The activities of 100 % *S, K, NaM* and *CaM* were 0.57, 0.95, 2.61, and 4.73, respectively. In *NaM-S* and *NaM-K* mixtures, the activity decreased as the *NaM* ratio decreased.

4.2. Undrained shear strength-cone penetration-water content relationship

One of the first experimental studies to determine the relationships between the undrained shear strength, cone penetration, and consistency of fine-grained soils was conducted by Hansbo [18]. According to his experimental test results, Hansbo [18] proposed Equation (1) based on the relationship between the cone penetration and undrained shear strength. Many researchers have proposed empirical equations between the cone penetration and undrained shear strength by performing a regression analysis based on a large amount of data [23, 35, 36]. Figure 5 shows the cone penetration (d)-undrained shear strength (S_u) relationship proposed by the authors on a log-log scale. The following equation was derived by assessing the experimental results):

$$S_u = 667{,}08 \cdot (d)^{-2} \tag{7}$$

The results shown in Figure 5 demonstrate that the cone penetration-undrained shear strength relationship has limited scatter within a small cone penetration range. Interestingly, the experimental results show that soil behaviour is independent of the soil physical properties, such as Atterberg limits, plasticity values, and grain size distribution.

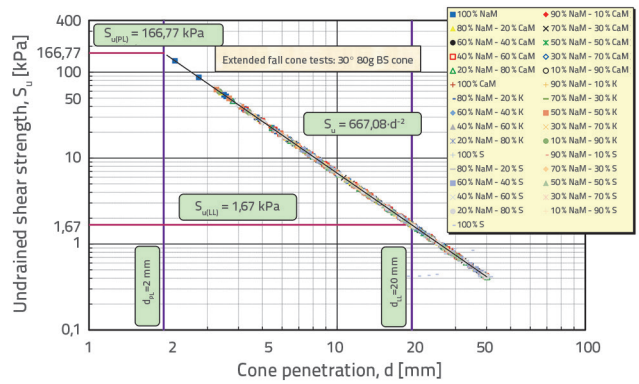

Figure 5. Cone penetration-undrained shear strength relationship for NaM-CaM, NaM-K, and NaM-S mixtures

Figure 6 shows the log-log plots of the water content and undrained shear strength of *NaM-CaM*, *NaM-K,* and *NaM-S* mixtures. The power function shown in Equation (8) is the most appropriate relation for describing the relationship between the water content and undrained shear strength [17, 28, 37].

$$S_u = A \cdot (w)^B \tag{8}$$

where A is a constant and B is the slope of the curve. As shown in Figure 6, *NaM-CaM* mixtures have much higher undrained shear strength values than the *NaM-K* and *NaM-S* mixtures. The lowest and highest water contents were obtained for *NaM-S* and *NaM-CaM* mixtures, respectively. The experimental results

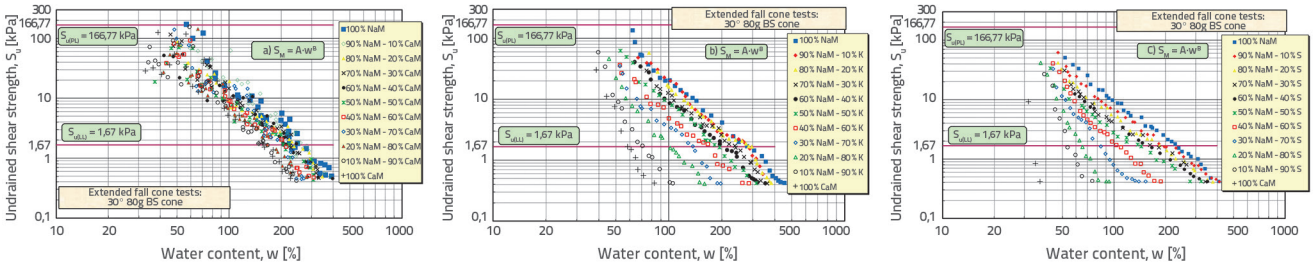

Figure 6. Undrained shear strength-water content relationship for a) NaM-CaM, b) NaM-K and c) NaM-S mixtures

showed that the undrained shear strength values of *NaM-CaM* mixtures are higher than those of *NaM-K* and *NaM-S* mixtures. Figure 6 shows that the mineralogical and plasticity properties affect the undrained shear strength values of soils. Figure 6 provides convenience in calculating the undrained shear strength corresponding to the desired water content of the clay-clay mixtures according to their plasticity properties.

The results shown in Figures 6a, 6b, and 6c can be easily understood by examining the changes in water content for each clay-clay mixture at a constant undrained shear strength value of 1.67 kPa. For example, as shown in Figure 6a, the water content at an undrained shear strength of 1.67 kPa for 100 % *NaM* is 248 % and that for 100 % *CaM* is 160 %. Figures 6b and 6c show that the water contents obtained for an undrained shear strength of 1.67 kPa for pure *K* and *S* are 58 % and 34 %, respectively. The water content values calculated above are also the LL values of the soils. This shows that when the water content corresponding to a constant undrained shear strength ($S_{u(LL)}$ = *1.67* kPa) is considered, the water contents required for *NaM-CaM, NaM-K,* and *NaM-S* mixtures are in descending order. The results showed that both mineralogical and consistency limits of the mixtures were significantly effective in varying the water-content-undrained shear strength.

4.3. Undrained shear strength-water content ratio relationship

A novel alternative solution is to indirectly obtain the undrained shear strength through regression analysis using the water content ratio (*WCR*) and liquidity index (I_L) of clays. Kuriakose et al. [12] expressed the water content ratio as the ratio of the water content to the LL. The I_L was obtained to calculate the distance from the natural water content of the clay soil samples to the liquid and plastic limits. The PL was obtained when the I_L value was zero, and the LL was obtained when the I_L value was one. If I_L values are less than zero, the water content of the soil is lower than the PL, whereas if it is greater than one, the water content of the soil is higher than the LL. Kuriakose et al. [12] demonstrated that using the water-content ratio is more appropriate than using I_L to determine the undrained shear strength of clay soils. The undrained shear strength -WCR relationships for *NaM-CaM, NaM-K* and *NaM-S* are shown in Figure 7. From the log (*WCR*)-log (S_u) graph plot shown in Figure 7, the undrained shear strength can be easily calculated using Equation (9) depending on the water content ratio (WCR).

$$S_u = F \cdot (WCR)^{\theta} \tag{9}$$

where *F* is a constant and θ is the slope of the line to the data points. In this study, Equations (10), (11), and (12) were used to obtain the S_u-*WCR* relationship for *NaM-CaM, NaM-K,* and *NaM-S* mixtures, respectively.

$$S_u = 1.873 \times (WCR)^{-2.449} (NaM - CaM) \tag{10}$$

$$S_u = 1.904 \times (WCR)^{-2.608} (NaM - K) \tag{11}$$

$$S_u = 1.838 \times (WCR)^{-3.068} (NaM - S) \tag{12}$$

The undrained shear strength values decreased with increasing water-content ratio up to 2. In the *NaM-CaM and NaM-K* mixtures, the undrained shear strength values decrease from 180 kPa to 0.4 kPa, while *WCR* values increase from 0.2 to 2, as shown in Figures 7a and 7b. Compared with the other two clay mixtures (*NaM-CaM, NaM-K*), in *NaM-S* mixtures with lower plasticity, undrained shear strength values decrease from 70 kPa to 0.4 kPa, while *WCR* values are increase from 0.2 to 2 as shown in Figure 7c.

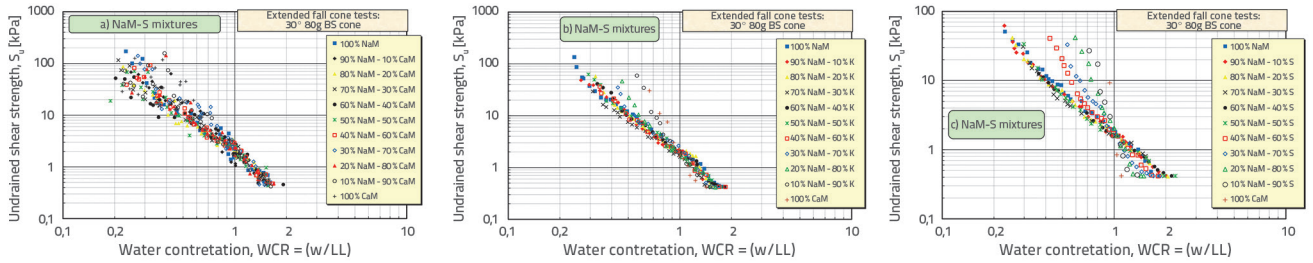

Figure 7. Undrained shear strength and water content ratio relationship for a) NaM-CaM, b) NaM-K and c) NaM-S mixtures

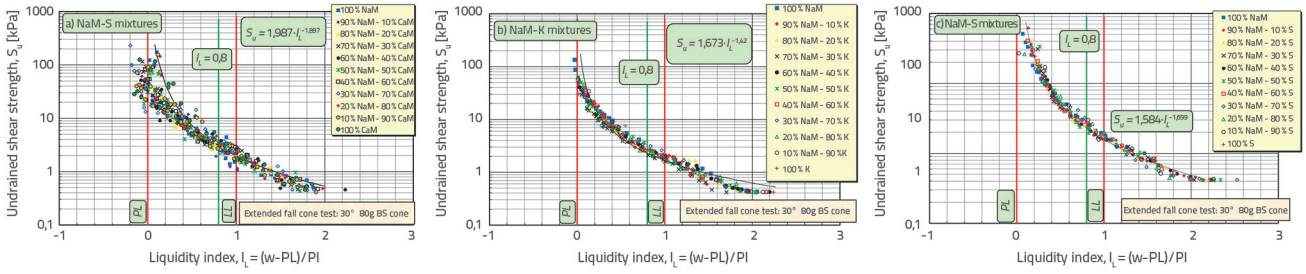

Figure 8. Undrained shear strength-liquidity index (IL) relationship for a) NaM-CaM, b) NaM-K and c) NaM-S mixtures

Additionally, as the *NaM* ratio in the mixtures decreased, the slope of the best-fit lines (Equations 10–12) increased. In this case, for a constant undrained shear strength (S_u = 10 kPa) the *WCR* values for 100 % *NaM* and *CaM* are 0.50 and 0.59, respectively. Figure 7b clearly shows that for an S_u value of 10 kPa, the required *WCR is 0.50* for 100 % *NaM*, whereas the *WCR* value increases to 0.83 for 100 % *K*. Mixtures of clays with close *LL* values in Figure 7a show that, at a constant undrained shear strength (S_u = 10 kPa), the difference between the *WCR* values is insignificant. Finally, in Figure 7c, the *WCR* values corresponding to an undrained shear strength of 10 kPa are 0.50 and 1.01 for 100 % *NaM* and *S*, respectively. Additionally, owing to the low *LL* values, *WCR* values slightly surpassed a value of 2 with increasing sepiolite content in the *NaM-S* mixtures (Figure 7c). Therefore, the experimental test results demonstrate good correlations obtained with regression analyses, which aids in obtaining the undrained shear strength of clay-clay mixtures more accurately and reliably based on the water content ratio.

If *WCR* is greater than 0.8, then clay is classified as 'soft loam and a difficult subgrade material' [49]. According to the test results and considering Equations (10) to (12), the θ values decrease with increasing *LL* and decreasing plasticity ratio (*PL/LL*). Therefore, it is evident that the plasticity ratio (*PL/LL*) or consistency characteristics substantially influence the S_u-*WCR* relationship. Equations (10) to (12) proposed in this study necessitates use of a *WCR* value between 0.8 and 2.

4.4. Undrained shear strength- liquidity index relationship

The undrained shear strength can be calculated easily using Equation (13) based on the liquidity index (I_L).

$$S_u = D \cdot (I_L)^{\lambda} \tag{13}$$

where *D* is a constant and λ is the slope of the line. Figure 8 shows the relationship between S_u-I_L and the *NaM-CaM, NaM-K* and *NaM-S* mixtures. Figure 8a shows that the *NaM-CaM* mixtures had a wider range of distribution than the *NaM-K* and *NaM-S* mixtures.

As shown in Equation (2), when the natural water content is equal to the plastic and LLs, I_L is equal to zero and one, respectively. Figure 8 shows the *LL* and *PL* boundaries of all three mixtures. It can easily be inferred that in *NaM-CaM* mixtures with very high plasticity, the I_L was less than 0; however, similar behaviour was not observed in *NaM-K* and *NaM-S* mixtures, which have much lower plasticity.

There are many equations proposed by researchers in the literature using clay minerals with different properties [11, 28, 30, 34, 37, 39, 50, 51]. Therefore, the analysis of the test data on different clay mixtures revealed that a unique relationship between S_u and I_L does not exist (Figures 8a–8c). Figure 8c shows the correlation between S_u and I_L for the *NaM-S* mixtures. Figure 8c shows a more uniform path than that shown in Figure 8a. In addition, a green I_L = *0.8* line has been added to Figure 8 for classification, which is one of the engineering properties of soils [49, 51, 52]. Experimental results, on the physical meaning of this value, S_u at I_L = *0.8* varies between about 1.8 and 2.2 times that of *LL* (Equation 14).

$$1{,}8 \cdot S_{u,LL} \le S_{u,(I_L = 0{,}8)} \le 2{,}2 \cdot S_{u,LL} \tag{14}$$

4.5. Undrained shear strength-liquidity index-sensitivity ratio relationships

The liquidity index (I_L) and sensitivity ratio (S_t) can be used together as a function to calculate the undrained shear strength of cohesive soils as follows [47]:

$$S_{u,c} = f(I_L, S_t) = 98 \times S_t \times e^{\left\{\frac{\ln\left(\frac{0.4755}{0.5012 + 0.4988 \times I_L}\right)}{0.19}\right\}} \tag{15}$$

When the sensitivity ratio is equal to one in Equation (15), the undrained shear strength can be obtained for the remoulded soils. Considering the mixtures of *NaM-CaM*, *NaM-K*, and *NaM-S*, the correlations between the liquidity index and undrained shear strength were obtained based on the sensitivity ratio. Furthermore, I_L-S_U-S_t relationship provides a general overview of the strength properties of these mixtures. In this case, the sensitivity ratio, which is affected by the sedimentary environment, mineralogical composition, and structure of clays, can also be associated with the liquidity index values. In Equation (15), S_u-I_L relationships for S_t = 1 are individually shown for *NaM-*

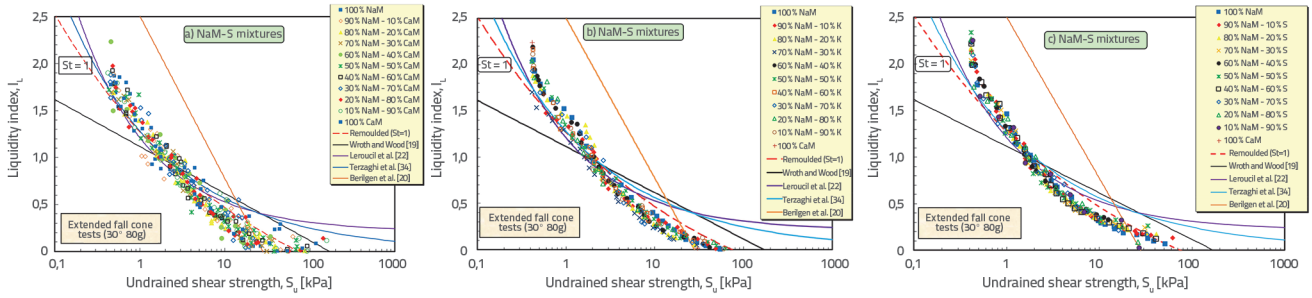

Figure 9. Undrained shear strength-liquidity index relationship for a) NaM-CaM, b) NaM-K and c) NaM-S mixtures

CaM, NaM-K and *NaM-S* mixtures (Figure 9.a to 9.c). As shown in all three graphs, when I_L is greater than 2.0, the corresponding S_u values remain constant as the I_L value increases. Moreover, in Equation (15), when I_L equal to one (at LL), $(S_u)_{LL}$ is equal to 1.91 kPa, 1.90 kPa, and 1.87 kPa and when I_L equal to zero (at PL), $(S_u)_{PL}$ is equal to 54.16 kPa, 61.66 kPa, and 82.05 kPa for *NaM-CaM, NaM-K,* and *NaM-S* mixtures, respectively. These results agree with those reported in literature [36, 47]. For example, the undrained shear strength values corresponding to the PL obtained by Li [53], Zentar et al. [54] and Shimobe and Spagnoli [47] are 71.2 kPa, 65 kPa, and 74.3 kPa, respectively, and these values are in good agreement with the values obtained in this study. The relationship between the liquidity index and undrained shear strength proposed by various researchers [19, 22, 30, 34] based on tests on remoulded soils with different mineralogical properties from different regions of the world are shown in Figure 9. By analysing the S_u-I_L plot, it is evident that the equation proposed by Berilgen et al. [30] overestimates the strength of the clay mixtures (Figure 9). When the undrained shear strength is less than 30 kPa, the equation calculates higher liquidity index values. When the equation proposed by Wroth and Wood [19] was used, the obtained liquidity index values were considerably lower than the experimental results when the undrained shear strength was extremely low. In addition, above a certain undrained shear strength value (S_u>2 kPa), this equation overestimates the liquidity index values. Compared to the equations of Berilgen et al. [30] and Wroth and Wood [19], the equations of Terzaghi et al. [34] and Leroueil et al. [22] appear to be in better agreement with the experimental results. In contrast, Terzaghi et al. [34] and Leroueil et al. [22] equations overestimate the liquidity index values, particularly at higher values of undrained shear strength. In this case, it was ascertained that the equation proposed by Shimobe and Spagnoli [47] was the most suitable.

4.6. Average undrained shear strengths of specimens at liquid and plastic limits

The undrained shear strengths obtained from the liquid and plastic limits of *NaM-CaM, NaM-K* and *NaM-S* mixtures are presented by incorporating the experimental results from literature, as shown in Figure 10 [17, 20, 28, 55]. The average $(S_u)_{LL}$ and $(S_u)_{PL}$ for *NaM-CaM* mixtures are 1.90 kPa and 130.55 kPa, respectively, whereas those for *NaM-K* mixtures were 1.94 kPa and 104.30 kPa, respectively. Finally, the average $(S_u)_{LL}$ and $(S_u)_{PL}$ for *NaM-S* mixtures are 1.83 kPa and 205.23 kPa, respectively. The undrained shear strength from higher to lower was obtained by testing *NaM-CaM, NaM-K,* and *NaM-S* mixtures. In addition, the

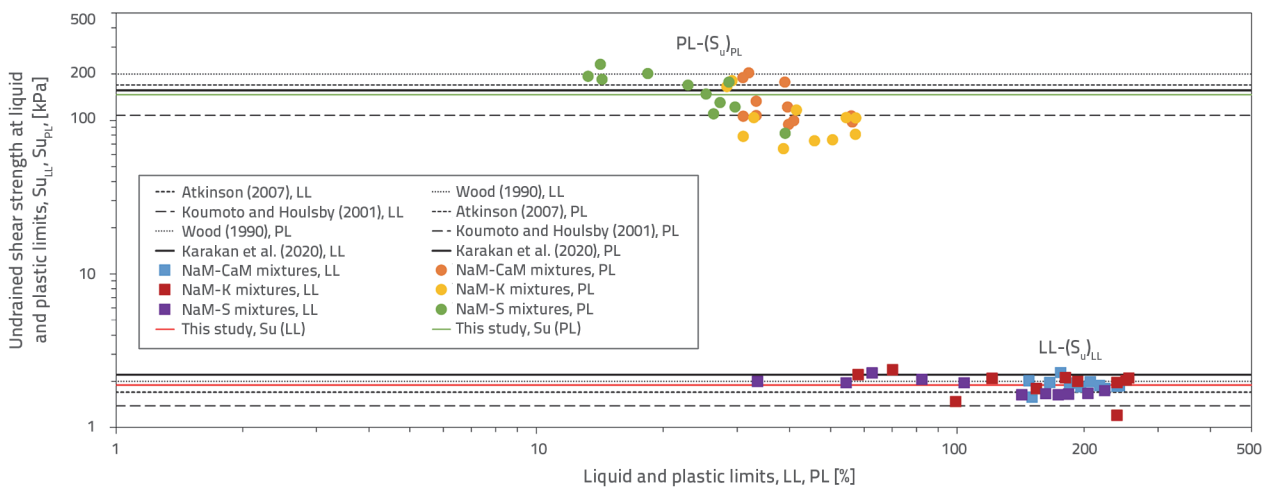

Figure 10. Undrained shear strengths at liquid and plastic limits for NaM-CaM, NaM-K and NaM-S mixtures (data obtained using Fall cone tests)

average undrained shear strengths of the clay-clay mixtures at their plastic and liquid limits are 166.77 kPa and 1.67 kPa, respectively.

Wood [20] stated that the undrained shear strength of kaolin-sand mixtures in the PL was lower than that of montmorillonite-sand mixtures. The $(S_u)_{LL}$ were at a maximum of 2.36 kPa and a minimum of 1.20 kPa, and the difference between them ($\Delta(S_u)_{LL}$) was 1.16 kPa (Figure 10). However, the $(S_u)_{PL}$ were obtained as maximum 425 kPa and minimum 65.16 kPa and the difference between them ($\Delta(S_u)_{PL}$) as 359.84 kPa (Figure 10). In this case, while the $\Delta(S_u)_{LL}$ of the *NaM-CaM, NaM-K,* and *NaM-S* mixtures is less significant, that of the $\Delta(S_u)_{PL}$ is substantially significant.

5. Conclusions

In this study, the influence of clay mineralogy on the interrelationships among *LL, PL, WCR,* S_u and I_L was investigated. Three types of clay (*CaM, K* and *S*) mixtures were blended with *NaM* to obtain soils with different plasticity characteristics. *NaM* was mixed with the three types of clay at 11 different concentrations ranging between 0 % and 100 % in increments of 10 % by weight.

The analysis of the results revealed that the LL values of the *NaM-S* mixtures decreased substantially as the *S* content in the mixture increased. Moreover, both the mineralogical properties and consistency limits of the mixtures were significantly effective in varying the water-content-undrained shear strength. In addition, given the large amount of data for the undrained shear strength values of *NaM*-clay mixtures, the relationship between the undrained shear strength and water content ratio was not unique. According to the obtained results, the undrained shear strength-liquidity index relationships for different clay mixtures were less affected by clay mineralogy and were more coherent than the undrained shear strength-water content ratio relationships of the same mixtures. For future work, the empirical equations proposed in this study should be verified using the test data on soils from different parts of the world.

REFERENCES

[1] Kumar, G.V., Wood, D.M.: Fall cone and compression tests on clay±gravel mixtures, Géotechnique., 49 (1999) 6, pp.727-739. https://doi.org/10.1680/geot.1999.49.6.727

[2] Mitchell, JK., Soga, K.: Fundamentals of soil behavior, John Wiley and Sons, 2005.

[3] Kashani, M.M., Hin, L.S., Ibrahim, S.B., Sulaiman, N.M.B.N., Teo, F.Y.: An investigation into the effects of particle texture, water content and parallel plates" diameters on rheological behavior of fine sediment, Int J Sediment Res., 31 (2016), pp.120–130. https://doi.org/10.1016/j.ijsrc.2015.11.001

[4] Kimiaghalam, N., Clark, S.P., Ahmari, H.: An experimental study on the effects of physical, mechanical and electrochemical properties of natural cohesive soils on critical shear stress and erosion rate, Int. J. Sediment Res., 31 (2016) 1, pp. 1–15. https://doi.org/10.1016/j.ijsrc.2015.01.001

[5] Tanzadeh, R., Vafaeian, M., Fard, M.Y.: The influence of lime powder on the behaviour of clay soil, GRAĐEVINAR, 73 (2021) 9, pp. 907-915, doi: https://doi.org/10.14256/JCE.1871.2016

[6] Abdulhussein Saeed, K., Kassim, K.A., Nur, H.: Physicochemical characterization of cement treated kaolin clay, GRAĐEVINAR, 66 (2014) 6, pp. 513-521, doi: https://doi.org/10.14256/JCE.976.2013

[7] British Standards Institute (BSI) BS 1377-2: Methods for test of soils for civil engineering purposes: Classification tests, British Standards Institute, London, United Kingdom, 1990.

[8] Sherwood, P.T., Ryley, M.D.: An investigation of a cone-penetrometer method for the determination of liquid limit, Géotechnique, 20 (1970) 2, pp. 203-208. https://doi.org/10.1680/geot.1970.20.2.203

[9] Wood, D.M.: Cone penetrometer and liquid limit, Géotechnique, 32 (1982) 2, pp. 152-157. https://doi.org/10.1680/geot.1982.32.2.152

[10] Nagaraj, H.B., Sridharan, A., Mallikarjuna, H.M.: Re-examination of Undrained Strength at Atterberg Limits Water Contents, Geotechnical and Geological Engineering, 30 (2012) 4, pp. 727-736. https://doi.org/10.1007/s10706-011-9489-7

[11] Vardanega, P.J., Haigh, S.K.: The undrained strength – liquidity index relationship. Canadian Geotechnical Journal, 51 (2014) 9, pp. 1073-1086. https://doi.org/10.1139/cgj-2013-0169

[12] Kuriakose, B., Abraham, B.M., Sridharan, A., Jose, B.T.: Water content ratio: an effective substitute for liquidity index for prediction of shear strength of clays, Geotech Geol Eng, 35 (2017) 4, pp.1577-1586. https://doi.org/10.1007/s10706-017-0193-0.

[13] O'Kelly, B.C.: Fall-cone strength testing of municipal sludges and residues, Environmental Geotechnics, 5 (2018)1, pp. 18-30. https://doi.org/10.1680/jenge.15.00080.

[14] Karakan, E., Demir, S.: Effect of fines content and plasticity on undrained shear strength of quartz-clay mixtures, Arab J Geosci., 11 (2018) 23, https://doi.org/10.1007/s12517-018-4114-1.

[15] Karakan, E., Demir, S.: Relationship between undrained shear strength with Atterberg limits of kaolinite/montmorillonite–quartz mixtures, Uluslararası Mühendislik Araştırma ve Geliştirme Dergisi, 10 (2018) 3, pp. 92–102.

[16] Karakan, E., Demir, S.: Observations and findings on mechanical and plasticity behavior of sand-clay mixtures, Arab J Geosci, 13 (2020), https://doi.org/10.1007/s12517-020-05762-4.

[17] Karakan, E., Shimobe, S., Sezer, A.: Effect of clay fraction and mineralogy on fall cone results of clay–sand mixtures, Eng Geol, 279 (2020), https://doi.org/10.1016/j.enggeo.2020.105887.

[18] Hansbo, S.: A new approach to the determination of shear strength of clay by the fall cone test, Proceedings of the Royal Swedish Geotechnical Institute, 14 (1957), pp. 5-47.

[19] Wroth C.P., Wood, D.M.: The correlation of index properties with some basic engineering properties, Canadian Geotechnical Journal, 15 (1978) 2, pp. 137-145. https://doi.org/10.1139/t78-014

[20] Wood, D.M.: Soil behaviour and critical state soil mechanics, Cambridge University Press, UK., 1990.

[21] Koumoto, T., Houlsby, GT.: Theory and practice of the fall cone test, Géotechnique, 51 (2001) 8, pp. 701-712. https://doi.org/10.1680/geot.2001.51.8.701

[22] Leroueil, S., Tavenas, F., Le Bihan, J.P.: Proprie´te´s caracte´ristiques des argiles de l"est du canada (Characteristic properties of eastern Canada clays), Can Geotech J., 20 (1983) 4, pp. 681–705. https://doi.org/10.1139/t83-076

[23] Federico, A.: A comment on undrained residual strength, Rivista Italiana di Geotecnica, 17 (1983) 3, pp. 164-166.

[24] Skempton, A.W., Northey, R.D.: The sensitivity of clays, Géotechnique, 3 (1952) 1, pp. 30–53. http://dx.doi.org/10.1680/geot.1952.3.1.30

[25] Schofield, A.N., Wroth, C.P.: Critical state soil mechanics, McGraw Hill, London,1968.

[26] Locat, J., Demers, D.: Viscosity, yield stress, remolded strength, and liquidity index relationships for sensitive clays, Can Geotech J., 25 (1988) 4, pp. 799–806. https://doi.org/10.1139/t88-088

[27] Yilmaz, I.: Evaluation of shear strength of clayey soils by using their liquidity index, Bull. Eng. Geol. Env., 59 (2000) 3, pp. 227–229. https://doi.org/10.1007/s100640100109

[28] Whyte, I.L.: Soil plasticity and strength: a new approach using extrusion, Ground Eng, 15 (1982) 1, pp. 16–20.

[29] Lee, L.T.: Predicting geotechnical parameters for dredged materials using the slump test method and index property correlations. DOER Technical Notes collection (ERDC TNDOER-D-1), U.S. Army Engineer Research and Development Center, Vicksburg,Mississippi, 2004. http://www.wes.army.mil/el/dots/doer

[30] Berilgen, S.A., Kılıc, H., Özaydın, K.: Determination of undrained shear strength for dredged golden horn marine clay with laboratory tests, Proceedings of the Sri Lankan geotechnical society"s first international conference on soil & rock engineering, Colombo, Sri Lanka, 2007.

[31] Edil, T.B., Benson, C.H.: Comparison of basic laboratory test results with more sophisticated laboratory and in situ tests methods on soils in southeastern Wisconsin, Final report of Wisconsin highway research program #0092-06-05, pp. 11–12, 2009.

[32] Tanzadeh, R., Vafaeian, M., Fard, M.Y.: The influence of lime powder on the behaviour of clay soil, GRAĐEVINAR, 73 (2021) 9, pp. 907-915, https://doi.org/10.14256/JCE.1871.2016

[33] Lebo, Ž., Bačić, M., Jurić-Kaćunić, D., Kovačević, M.S.: Zagreb clay improved with various binders, GRAĐEVINAR, 73 (2021) 9, pp. 871-880, https://doi.org/10.14256/JCE.3300.2021.

[34] Terzaghi, K., Peck, R.B., Mesri, G.: Soil mechanics in engineering practice, 3rd edn. John Wiley & Sons, New York 1996.

[35] Shimobe, S.: Correlations among liquidity index, undrained shear strength and fall cone penetration of fine-grained soils, In: Proc. Of Coastal Geotechnical Engineering in Practice, Balkema, Rotterdam (the Netherlands), pp. 141–146, 2000.

[36] Shimobe, S.: Determination of index properties and undrained shear strength of soils using the fall-cone test, In: Proceeding of the 7th International Symposium on Lowland Technology, pp.16-18, 2010.

[37] O'Kelly, B.C.: Atterberg limits and remolded shear strength – water content relationships, Geotech Test J., 36 (2013) 6, pp. 939–947. https://doi.org/10.1520/GTJ20130012.

[38] Cangir, B., Dipova, N.: Estimation of undrained shear strength of Konyaalti silty clays, Indian J Geo Mar Sci., 46 (2017) 3, pp. 513–520.

[39] Kang, G., Tsuchida, T., Tang, T.X., Kalim, T.P.: Consistency measurement of cement-treated marine clay using fall cone test and Casagrande liquid limit test, Soils Found., 57 (2017) 5, pp. 802–814. https://doi.org/10.1016/j.sandf.2017.08.010

[40] Sharma, B., Sridharan, A.: Liquid and plastic limits of clays by cone method, Int J Geo-Eng., 9 (2018) 1,pp. 22–31. https://doi.org/10.1186/s40703-018-0092-0

[41] Di Matteo, L.: Liquid limit of low- to medium-plasticity soils: comparison between Casagrande cup and cone penetrometer test, Bulletin of Engineering Geology and the Environment, 71 (2012) 1, pp. 79-85. https://doi.org/10.1007/s10064-011-0412-5

[42] Feng, T.W.: Fall-cone penetration and water content relationship of clays, Géotechnique, 50 (2000) 2, pp. 181-187. https://doi.org/10.1680/geot.2000.50.2.181

[43] Sivakumar, G.V., Glynn, D., Cairns, P., Black, J.A.: A new method of measuring plastic limit of fine materials, Géotechnique, 59 (2009) 10, pp. 813-23. https://doi.org/10.1680/geot.2011.61.1.88

[44] Spagnoli, G.: Comparison between Casagrande and drop-cone methods to calculate liquid limit for pure clay, Canadian Journal of Soil Science, 92 (2012) 6, pp. 859-64. https://doi.org/10.4141/cjss2012-011

[45] Hong, Z., Liuz, S., Shen, S., Negami, T.: Comparison in Undrained Shear Strength between Undisturbed and Remolded Ariake Clays, J Geotech Geoenv Eng, 132 (2006) 2, pp. 272–275. https://doi.org/10.1061/(ASCE)1090-0241(2006)132:2(272)

[46] O'Kelly, B.C., Vardanega P.J., Haigh, S.K.: Use of fall cones to determine Atterberg limits: a review, Géotechnique, 68 (2018) 10, pp. 843-856, Corrigendum, 935. https://doi.org/10.1680/jgeot.18.D.001

[47] Shimobe, S., Spagnoli, G.: Some relations among fall cone penetration, liquidity index and undrained shear strength of clays considering the sensitivity ratio, B Eng Geol Environ. 78 (2019) 7, pp. 5029–5038. https://doi.org/10.1007/s10064-019-01478-2

[48] Feng, T-W.: A linear log d – log w model for the determination of consistency limits of soils, Canadian Geotechnical Journal, 38 (2001) 6, pp. 1335-1342. https://doi.org/10.1139/t01-06

[49] So, E.: Statistical correlation between allophane content and index properties for volcanic cohesive soil, Soils Found., 38 (1998) 4, pp. 85–93. https://doi.org/10.3208/sandf.38.4_85

[50] Spagnoli, G., Oreste, P.: Relation water content ratio-to-liquidity index versus the Atterberg limits ratio evaluated with the Kaniadakis exponential law, Geomech Geoeng 14 (2019) 2, pp. 148–153. https://doi.org/10.1080/17486025.2018.1532117

[51] Shimobe, S., Spagnoli, G.: Relationships between undrained shear strength, liquidity index, and water content ratio of clays, Bull Eng Geol Environ, 79 (2020), pp. 4817–4828. https://doi.org/10.1007/s10064-020-01844-5.

[52] Moroto, N.: Basic properties of loam soils in Aomori prefecture, Japan, Soils Found., 33 (1993) 2, pp. 35–46. https://doi.org/10.3208/sandf1972.33.2_35

[53] Li, K.: A study of determining properties of fine-grained soil by fall cone test. Master thesis, Chung Yuan Christian University, 2004.

[54] Zentar, R., Abriak, N.E., Dubois, V.: Fall cone test to characterize shear strength of organic sediments, J Geotech Geoenviron, 135 (2009) 1, pp. 153–157. https://doi.org/10.1061/(ASCE)1090-0241(2009)135:1(153)

[55] Atkinson, J.: The mechanics of soils and foundations, CRC Press, London, 2007.